The Journal of Immunology

RESEARCH ARTICLE | AUGUST 15 2002

DNA Methylation Changes at Human Th2 Cytokine Genes Coincide with DNase I Hypersensitive Site Formation During CD4+ T Cell Differentiation[1] FREE

Samantha Santangelo; ... et. al

J Immunol (2002) 169 (4): 1893–1903.
https://doi.org/10.4049/jimmunol.169.4.1893

DNA Methylation Changes at Human Th2 Cytokine Genes Coincide with DNase I Hypersensitive Site Formation During CD4$^+$ T Cell Differentiation[1]

Samantha Santangelo, David J. Cousins, Nicole E. E. Winkelmann, and Dontcho Z. Staynov[2]

The differentiation of naive CD4$^+$ T lymphocytes into Th1 and Th2 lineages generates either cellular or humoral immune responses. Th2 cells express the cytokines IL-4, -5, and -13, which are implicated in asthma and atopy. Much has been published about the regulation of murine Th2 cytokine expression, but studies in human primary T cells are less common. We have developed a method for differentiating human CD45RA$^+$ (naive) T cells into Th1 and Th2 populations that display distinct cytokine expression profiles. We examined both CpG methylation, using bisulfite DNA modification and sequencing, and chromatin structure around the *IL-4* and *IL-13* genes before and after human T cell differentiation and in normal human skin fibroblasts. In naive cells, the DNA was predominantly methylated. After Th2 differentiation, DNase I hypersensitive sites (DHS) appeared at *IL-4* and *IL-13* and CpG demethylation occurred only around the Th2-specific DHS. Both DHS and CpG demethylation coincided with consensus binding sites for the Th2-specific transcription factor GATA-3. Although fibroblasts, like naive and Th1 cells, did not express IL-4 or IL-13, DHS and unmethylated CpG sites that were distinct from the Th2-specific sites were observed, suggesting that chromatin structure in this cluster not only varies in T cells according to IL-4/IL-13 expression but is also tissue specific. *The Journal of Immunology*, 2002, 169: 1893–1903.

During CD4$^+$ T lymphocyte differentiation, at least two distinct subsets of cells, Th1 and Th2, are derived from antigenically naive precursors, depending on the nature of the pathogen or allergen encountered (1, 2). These subsets are characterized by the different arrays of cytokines that they secrete on activation. Th1 cells express IFN-γ and TNF-β and regulate cell-mediated immunity against intracellular pathogens. Th2 cells express IL-4, -5, and -13, which promote Ab-mediated (humoral) responses and eosinophil-mediated effects (1) and are also implicated in asthma and atopy (3). The major factor that determines the commitment of naive T cells to either the Th1 or the Th2 lineage is exposure to IL-12 or IL-4, respectively. This process has been extensively investigated in mice (4). In Th1 cells, signals from the IL-12R activate the STAT4 pathway, which, together with signals from the TCR and the transcription factor T-bet, plays a role in activating IFN-γ expression (5, 6). In Th2 cells, signals from the IL-4R activate the STAT6 pathway, leading to the activation of many IL-4-regulated genes (7). Two Th2-specific transcription factors have been identified: c-Maf and GATA-3 (8, 9). c-Maf activates IL-4 expression (10) and GATA-3 regulates IL-4, -5, and -13 expression (11, 12).

The genes encoding the human Th2 cytokines IL-4 and IL-13 are located on the long arm of chromosome 5 between the ubiquitously expressed genes *KIF3A* and *RAD50* (see Fig. 1*A*) (13). The organization of the murine *IL-4/IL-13/IL-5* locus is similar to that of the human locus, and a 401-bp noncoding sequence that is conserved between humans and mice, termed conserved noncoding sequence-1 (CNS-1),[3] is found between *IL-4* and *IL-13* (14). It has recently been suggested that CNS-1 is a coordinate regulator of *IL-4*, *IL-5*, and *IL-13* (15). Chromatin studies in murine T cells have shown that Th2 differentiation from naive cells is accompanied by the appearance of Th2-specific DNase I hypersensitive sites (DHS) around the *IL-4* and *IL-13* genes (16, 17). Because most of these DHS were not seen in naive or Th1 cells, it was proposed by Agarwal and Rao (16) that the chromatin is "closed" in naive cells, and that after Th2 cell differentiation the chromatin structure of the *IL-4/IL-13* cluster "opens" to enable the expression of these cytokines.

Chromatin structure is linked to the methylation status of the cytosines in CpG dinucleotides (18). Changes in CpG methylation patterns have been found to correlate with several processes within the murine immune system, including Ig κ-chain rearrangement during B lymphocyte differentiation (19), TCR-β chain rearrangement (20), and *IL-3* and *IFN-γ* transcription during CD8$^+$ T lymphocyte differentiation (21, 22). Limited CpG methylation analysis of the murine *IL-4* and *IL-5* genes using methylation-sensitive restriction enzymes has led to reports that the DNA in *IL-4* and *IL-5* is methylated in naive and Th1 cells but becomes demethylated in Th2 cells (16, 23). More recently, T cell-specific deletion of the DNA methyltransferase Dnmt1 resulted in decreased methylation and increased activation-induced expression of several cytokines in naive murine T cells, suggesting that CpG methylation plays an important role in limiting the expression of these genes in naive cells (24).

The chromatin structure and DNA methylation status of *IL-4* and *IL-13* have not been previously studied in human T cells. In this work we show that Th2-specific DHS appear in the second intron of *IL-4*, around the *IL-13* promoter and near (but not in) CNS-1 after 14 days of human CD4$^+$ T cell differentiation. These

Department of Respiratory Medicine and Allergy, King's College, London, United Kingdom

Received for publication February 20, 2002. Accepted for publication June 4, 2002.

The costs of publication of this article were defrayed in part by the payment of page charges. This article must therefore be hereby marked *advertisement* in accordance with 18 U.S.C. Section 1734 solely to indicate this fact.

[1] This work was supported by Medical Research Council Grant G9815922.

[2] Address correspondence and reprint requests to Dr. Dontcho Z. Staynov, Department of Respiratory Medicine and Allergy, King's College, Fifth Floor Thomas Guy House, Guy's Hospital, London SE1 9RT, U.K. E-mail address: dontcho.staynov@kcl.ac.uk

[3] Abbreviations used in this paper: CNS-1, conserved noncoding sequence-1; DHS, DNase I hypersensitive site; BSM, bisulfite-modified.

0022-1767/02/$02.00

DHS coincide with several regions of regulatory interest in murine Th2 cytokine genes. This is also the first in-depth analysis, using bisulfite DNA modification and sequencing, of the CpG methylation status across the *IL-4* and *IL-13* genes before and after differentiation. In Th2 cells, CpG demethylation was not the locus-wide event reported to occur in the murine Th2 cytokine cluster (25) but occurred only around DHS. We compared DHS and CpG methylation patterns in T cells with those in normal human skin fibroblasts, a nonhemopoietic lineage, and found that the DNA around *IL-4* and *IL-13* in nonexpressing cells is neither fully methylated nor insensitive to DNase I digestion, in contrast to previous reports (16, 17, 23). Chromatin structure and DNA methylation status differ between hemopoietic (T cells) and nonhemopoietic (fibroblasts) cells, suggesting that they are tissue specific.

Materials and Methods

Cells and tissue culture

Venous blood was taken from nonatopic healthy human male volunteers using heparin as an anticoagulant. Ethical approval for the use of human volunteers in this study was obtained from the institutional ethical review committee. PBMCs were isolated using Lymphoprep (Nycomed, Oslo, Norway) according to the manufacturer's instructions. $CD4^+$ T cells were isolated from PBMC using a CD4 Positive Isolation kit (Dynal Biotech, Oslo, Norway) according to the manufacturer's instructions. Naive $CD45RA^+$ cells were purified from $CD4^+$ cells by depletion of $CD45RO^+$ cells using mouse anti-human CD45RO Ab (UCHL1; 0.5 μg/1 $\times$ 10^6 cells; BD PharMingen, San Diego, CA) and rat anti-mouse IgG2a Dynabeads (Dynal Biotech) according to the manufacturer's instructions. The purity of fractionated cell populations was determined by FACS analysis using FITC-conjugated anti-CD45RA (L48; BD PharMingen), PE-conjugated anti-CD45RO (UCHL1; BD PharMingen), CyChrome-conjugated anti-CD4 (RPA-T4; BD PharMingen); FITC-conjugated anti-CD14 (MϕP9; BD PharMingen), and PE-conjugated anti-CD16 (3G8; BD PharMingen). Samples were analyzed on a FACSCalibur (BD Biosciences, Mountain View, CA).

Purified $CD45RA^+$ cells (1 $\times$ 10^6/ml) were cultured in RPMI 1640 (Life Technologies, Rockville, MD) supplemented with 10% FCS, 2 mM L-glutamine (Life Technologies), 100 U/ml penicillin (Life Technologies), and 100 μg/ml streptomycin (Life Technologies). Cells were stimulated with plate-bound anti-CD3 (1 μg/ml; clone OKT3) and anti-CD28 (2 μg/ml; clone 15E8; Central Laboratory of The Netherlands Red Cross Blood Transfusion Service, Amsterdam, The Netherlands), and rIL-2 (50 U/ml; Eurocetus, Amsterdam, The Netherlands). To direct Th1 differentiation, IL-12 (2.5 ng/ml; R&D Systems, Minneapolis, MN) and anti-IL-4 (5 μg/ml; clone MP4-25D2; BD PharMingen) were added. For Th2 differentiation, IL-4 (12.5 ng/ml; NBS Biologicals, Huntingdon, Cambridgeshire, U.K.), anti-IFN-γ (5 μg/ml; clone B-B1; BioSource International, Camarillo, CA), and anti-IL-10 (5 μg/ml; clone JES3-9D7; BioSource International) were added. After 4 days, the cells were expanded under the same conditions in the absence of anti-CD3 or anti-CD28. Cells were then restimulated every 7 days. When required, cells were activated with PMA (5 ng/ml; Sigma-Aldrich, St. Louis, MO) and ionomycin (500 ng/ml; Calbiochem, La Jolla, CA) for 4 h. After differentiation and before DHS analysis, dead cells were removed from the culture using the Dead Cell Removal kit (Miltenyi Biotec, Auburn, CA) according to the manufacturer's instructions.

Untransformed human fibroblasts from the skin of three normal males were obtained from the European Cell Culture Collection (ECACC; nos. 90011806, 90011807, and 90011810) (26). They were grown in MEM with Earle's salts (Life Technologies) supplemented with penicillin, streptomycin, and L-glutamine as above, 1$\times$ nonessential amino acids (Life Technologies), and 15% FCS. Where necessary, cells were activated with IL-1β, TNF-α, and IFN-γ (10 ng/ml each; R&D Systems) for 24 h.

DNA sequence and computational analysis

The contig shown in Fig. 1 was created from sequences deposited in the GenBank database (accession nos. AC004237, AC004039, AC004041, and AC004042) using MacVector version 6.5 (Oxford Molecular, Oxford, U.K.). Numbering throughout this report is from the start of sequence AC004237. Sequence analysis for restriction enzyme sites, CpG sites, and PCR primer design and sequence alignment was performed using MacVector. All DHS and CpG sites that are described in this paper are found between two *Eco*RI sites that are located at the 3′ end of *IL-4* and upstream of *IL-13*, respectively.

RT-PCR

Isolation of total cellular RNA and DNA was performed using the RNA/DNA Mini kit (Qiagen, Valencia, CA) according to the manufacturer's instructions and RT-PCR was performed as previously described (27) using 25 ng (T cells) or 500 ng (fibroblasts) of reverse-transcribed RNA. The primers used in RT-PCR for β-actin, KIF3A, IL-4, IL-13, and RAD50 have been described previously (27). RT-PCR primers for IFN-γ and GM-CSF were as follows: IFN-γ sense, 5′-GCAGGTCATTCAGATGTAGCGG; IFN-γ antisense, 5′-TGTCTTCCTTGATGGTCTCCACAC; GM-CSF sense, 5′-GCCAGCCACTACAAGCAGCAC; GM-CSF antisense, 5′-CAAAGGGGATGACAAGCAGAAAG. MWG Biotech (Ebersberg, Germany) supplied all primers.

The final number of PCR cycles was selected so that a clearly visible amplimer could be seen before the PCR reached product saturation (Fig. 1, *C* and *D*).

DNase I hypersensitivity analysis

DHS analysis of the T cells was performed using methods adapted from Cockerill (28). Briefly, T cell nuclei were prepared by washing cells in ice-cold PBS and resuspending them in lysis buffer (20 mM Tris (pH 7.5), 15 mM NaCl, 6 mM $MgCl_2$, 0.1% Nonidet P-40, 20% glycerol, 0.1 mM EDTA, 0.1 mM EGTA, and 0.1 mM PMSF). After a 6-min incubation on ice, the nuclei were washed twice with wash buffer (lysis buffer without Nonidet P-40) and once with DNase I digestion buffer (DDB) (wash buffer with 1 mM $CaCl_2$). The nuclei were resuspended in DDB before digesting equal aliquots with 10–26 U of DNase I (Sigma-Aldrich) at 25°C for 10 min. Fibroblast chromatin was digested with DNase I following cell permeabilization as described (29). After DNase I treatment, DNA was isolated using the DNeasy Tissue kit (Qiagen) according to the manufacturer's instructions.

DNase I-digested DNA was then digested with *Eco*RI or *Bcl*I and precipitated. Five micrograms per lane of restriction-digested DNA were electrophoresed through a 0.7% TAE agarose gel and Southern-blotted as described (30). Fragments to be used as probes in DHS analyses were amplified from genomic DNA using the following primers: *IL-4* DHS probe, 5′-CCAATCAGCACCTCTCTTCCAG and 5′-AACCTCAGAATAGACCTACCTTGCC; CNS-1 DHS probe, 5′-CAGTCCTCAGGAGATGTGATTGTG and 5′-GTCAGGAGAGGGGCAGAACAG; *IL-13* DHS probe, 5′-GACTCCTGGTGTCCACTGCTTTAG and 5′-TCAAAAATGTCTTGGGTAGGCG. Probes were radiolabeled with [α-^{32}P]dCTP or [α-^{32}P]dATP (3000 Ci/mmol) using the Prime-a-Gene Labeling System (Promega, Madison, WI) and prehybridization and hybridization, using ULTRAhyb (Ambion, Austin, TX), were conducted according to the manufacturer's instructions. DHS were mapped using at least two restriction enzymes, and their location was confirmed by probing both ends of the same parent fragment.

Bisulfite modification of DNA

CpG methylation was examined in DNA from T cells of two normal male volunteers and in DNA from untransformed fibroblasts of three normal males obtained from ECACC (see *Cells and tissue culture*) with similar results; all CpG methylation data presented in this report are from one of these individuals, respectively. The method for bisulfite modification of DNA was adapted from Frommer et al. (31). Ten micrograms of genomic DNA were digested with the restriction enzyme *Afl*III (New England Biolabs, Beverly, MA) to fragment the DNA. For sodium bisulfite modification, DNA was denatured in a final volume of 111 μl 0.3 M NaOH (Sigma-Aldrich) at 37°C for 15 min. To this was added 1.1 ml of bisulfite/hydroquinone solution (pH 5; 9.5 g sodium bisulfite (Sigma-Aldrich), 1.5 ml 3 M NaOH, and 2.5 ml 20 mM hydroquinone (Sigma-Aldrich) in a final volume of 20 ml). The samples were incubated in the dark at 55°C for 5 h. Salt was removed from the modified DNA using the Wizard DNA Clean-Up System (Promega) according to the manufacturer's instructions, and the DNA was eluted in 100 μl H_2O. The DNA was desulfonated in a final concentration of 0.3 M NaOH at 37°C for 15 min. The samples were neutralized by adding 1 volume of 6 M ammonium acetate (pH 7), and the DNA was precipitated with three volumes of 100% ethanol. The precipitated DNA was washed twice with 70% ethanol, dried, and resuspended in 100 μl EB buffer (10 mM Tris (pH 8.5); Qiagen).

PCR and sequencing of BSM DNA

Primers for the amplification of bisulfite-modified (BSM) DNA were designed to be specific for modified DNA only and are as follows: *IL-4*

promoter BSM-PCR, 5′-GTTTTGTGAGGTTGTTTAAAGTTTTGATG and 5′-CTAATTAACCCCAAATAACTAACAATC; *IL-4* DHS I and II BSM-PCR, 5′-GAGAAAATGTATTATTAGTTGTTAAATT and 5′-CATTTTATCTAAAAAACTTCCTATAAC; *IL-13* promoter BSM-PCR, 5′-TTGGGTGATGTTGATTAGTTTTTTAATGAG and 5′-CAAATCT TAAAAACTCTACCCTAAACCC. PCR were conducted under the following conditions: 400 ng BSM DNA, 1× PCR buffer II (PE Applied Biosystems, Foster City, CA), 3 mM $MgCl_2$, 0.2 mM dNTPs, 2.5 U AmpliTaq Gold (PE Applied Biosystems), and 1 μM of each primer in a final volume of 100 μl. Cycling conditions were as follows: 10 min at 95°C, followed by five cycles of 2 min at 95°C, 3 min at 60°C, and 3 min at 72°C, then a further 30–35 cycles of 1 min at 95°C, 1 min at 60°C, 1 min at 72°C, and a final 10-min extension step at 72°C. To test the specificity of the primers for modified DNA, the reactions were also performed using 400 ng unmodified, *Afl*III-digested human genomic DNA (Promega).

Direct sequencing of BSM-PCR products was performed using the Thermo Sequenase Radiolabeled Terminator Cycle Sequencing kit (Amersham Pharmacia Biotech, Piscataway, NJ) according to the manufacturer's instructions. The sequences were checked against those published, and the intensity of the C vs T bands on the autoradiographs was evaluated visually. PCR fragments were also cloned into the vector pCR 2.1 TOPO using the TOPO TA Cloning kit (Invitrogen, San Diego, CA) according to the manufacturer's instructions. Plasmid DNA was sequenced with the Big Dye DNA Sequencing kit (PE Applied Biosystems) according to the manufacturer's instructions, using the M13 forward and reverse primers. The reactions were analyzed on a PE Applied Biosystems 377 sequencing machine.

Restriction enzyme analysis of CpG methylation

Genomic DNA from activated and unactivated Th1 and Th2 cells and from fibroblasts was digested first with *Eco*RI, then with *Hpa*II or *Msp*I. The DNA was electrophoresed and Southern blotted as described above before hybridizing each region with up to five probes (data not shown) to enable accurate mapping of *Hpa*II site digestion.

Results

Differentiation of human Th1 and Th2 cells in vitro

The surface expression of different isoforms of CD45 can be used to distinguish naive $CD4^+$ T cells (which express CD45RA) from memory T cells (which express CD45RO) (32, 33). Therefore, $CD45RA^+$ T cells were purified from $CD4^+$ T cells to form the naive starting population (Fig. 1*B*, *top* and *middle panels*). After CD45RO depletion, the T cells were at least 98% $CD4^+CD45RA^+$ in all experiments. NK cells ($CD16^+$) or monocytes ($CD14^+$) represented <1% of the population (Fig. 1*B*, *bottom panels*).

The naive $CD4^+CD45RA^+$ T cells were differentiated to a Th1 (using IL-12 and anti-IL-4) or a Th2 (using IL-4, anti-IFN-γ, and anti-IL-10) phenotype. Cytokine expression was analyzed by RT-PCR before and after differentiation. $CD45RA^+$ cells stimulated

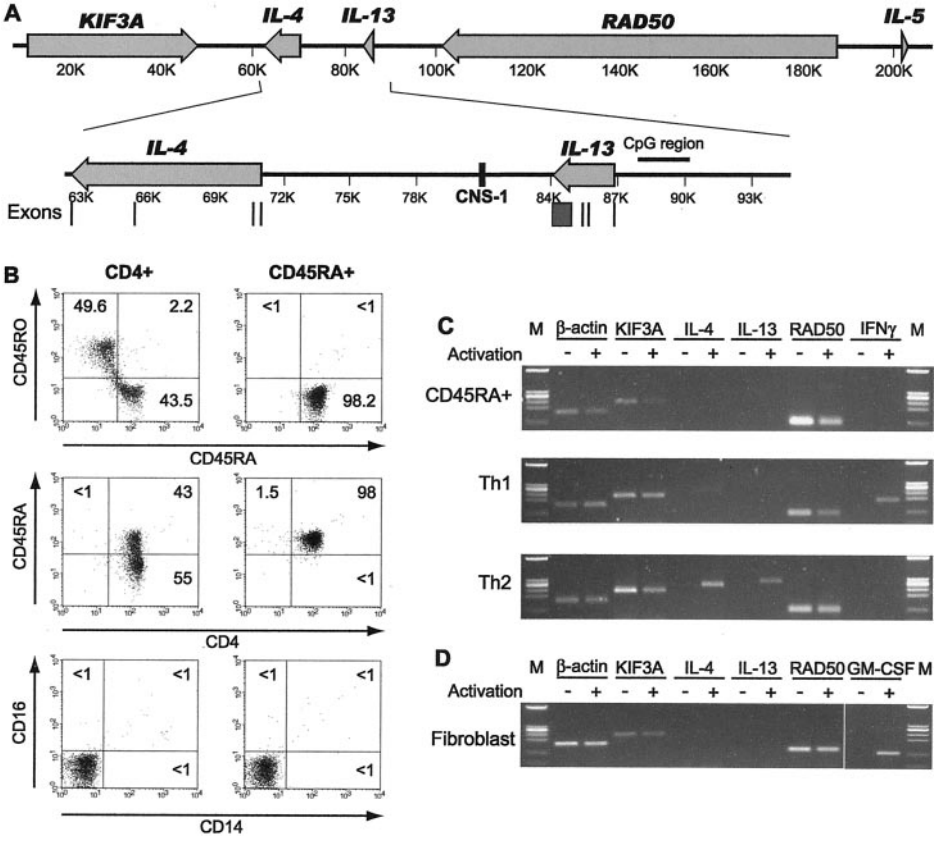

FIGURE 1. *A*, The Th2 cytokine gene cluster on human chromosome 5q. Arrows indicate the positions of the genes and the direction of transcription; numbers *below* the arrows designate scale in kilobases (K). The region analyzed in this report is detailed *below* the main map. Exons are depicted as shaded rectangles beneath the arrows. *B*, Expression of cell surface markers on $CD4^+$ and $CD45RA^+$ populations determined by multicolor immunofluorescence. Dot plots of one representative experiment (of five) are shown. Quadrant markers were set based on isotype-matched Abs as controls. Number in each quadrant indicates the percentage of positive cells. *C*, Differentiation toward Th1 or Th2 phenotypes after 14 days as assessed by RT-PCR. Cells were activated (+) with PMA and ionomycin where indicated. Relative expression was investigated in naive cells (*top panel*) and Th1 (*middle panel*) or Th2 (*bottom panel*) cells by amplifying mRNA as follows: β-actin, 22 cycles; KIF3A, 28 cycles; IL-4, 28 cycles; IL-13, 24 cycles; RAD50, 30 cycles; and IFN-γ, 18 cycles. Similar results were obtained from three independent experiments; the fragment size marker (M) was ϕ174 *Bsu*R I. *D*, Relative gene expression in fibroblasts. Cells were activated (+) with IL-1β, TNF-α, and IFN-γ where indicated. RT-PCR cycles were as follows: β-actin, 22 cycles; KIF3A, 27 cycles; IL-4, 38 cycles; IL-13, 38 cycles; RAD50, 27 cycles; and GM-CSF, 32 cycles.

with PMA and ionomycin for 4 h did not express IL-4, IL-13, or IFN-γ mRNA (Fig. 1*C*, *top panel*). Under the same conditions, the in vitro-differentiated Th1 cells expressed IFN-γ mRNA (Fig. 1*C*, *middle panel*) and the Th2 cells expressed IL-4 and IL-13 mRNA (Fig. 1*C*, *bottom panel*), indicating that, after 14 days in culture, the $CD4^+CD45RA^+$ cells had differentiated into either Th1 or Th2 populations. Transcription of KIF3A and RAD50 mRNA was also examined. KIF3A and RAD50 mRNAs were expressed constitutively in both naive and differentiated T cell populations (Fig. 1*C*), suggesting that these genes are regulated independently of IL-4 and IL-13. KIF3A and RAD50 were not up-regulated upon activation. Intracellular cytokine staining and FACS analyses (data not shown) indicated that <1% of the Th1 population expressed IL-4 and IL-13, while 90.8% of these cells expressed IFN-γ. Of the Th2 population, 19.8% of the cells expressed IL-4, 36.2% expressed IL-13, and 1.4% expressed IFN-γ (data not shown). IL-4 and IL-13 expression was not detected in fibroblasts, even upon activation (Fig. 1*D*). GM-CSF expression, which was used as an activation marker in fibroblasts, was detected only in the activated population.

DHS and CpG methylation in the IL-4 *gene*

Unactivated cells were used in this study so that differentiation-specific (as opposed to activation-specific) chromatin structure changes could be examined in the absence of active IL-4 and IL-13 transcription. DNase I hypersensitivity assays revealed three DHS in the *IL-4* gene in Th2 cells (Fig. 2*A*, *middle panel*, and *C*). The sites designated I, II, and III were ~1, 1.2, and 2.3 kb downstream of the *IL-4* transcription start site. The positions of DHS I and II were confirmed by comparing the position of the DHS bands with that of an *Eco*RI-Fse I fragment (data not shown). Therefore, the Th2-specific DHS were located in the second intron of *IL-4*, and DHS I and II coincided with several consensus GATA-3 binding sites (Fig. 2*E*). Very faint bands corresponding to DHS II and III are visible in the Southern blot of Th1 cell DNA (Fig. 2*A*, *left panel*). However, these are substantially weaker than the hypersensitive sites visible in Th2 DNA and may be caused by the activation of the *IL-4* locus in a small minority of cells in the Th1 population.

Two DHS were observed in fibroblast chromatin (Fig. 2*A*, *right panel*, and *C*). These DHS were distinct from those observed in Th2 chromatin: DHS FI is ~0.8 kb from the *IL-4* transcription site, i.e., just downstream of the second exon, and DHS FII is ~3.4 kb from the transcriptional start site. The presence of these fibroblast-specific DHS in *IL-4* was confirmed using fibroblasts from a second individual. $CD45RA^+$ naive T cells could not be analyzed by this method due to the large number of cells required. The appearance of DHS in the *IL-4* gene of both Th2 cells and fibroblasts was intriguing and prompted us to investigate CpG methylation across this gene in expressing and nonexpressing cell types.

Initially, we examined the *IL-4* gene by hybridizing DNA that had been digested with the methylation-sensitive restriction enzyme *Hpa*II to five radiolabeled probes that spanned the entire region (Fig. 2*B*, only one Southern blot is shown). Differences in *Hpa*II digestion between Th1 and Th2 cells were seen at two sites between the Th2-specific DHS I and II (Fig. 2, *B* and *D*, ∗). The unmethylated CpGs at these sites in Th2 cells thus coincided with the appearance of Th2-specific DHS; these CpG sites were methylated in Th1 cells. Activation did not affect CpG methylation at *Hpa*II sites in either Th1 or Th2 cells (Fig. 2*B*). Although fibroblasts do not express IL-4, the *IL-4* gene was not completely methylated at all CpG sites. Indeed, *Hpa*II digestion indicated that more CpG sites were unmethylated in these cells than in T cells (Fig. 2, *B* and *D*).

*Hpa*II digestion analysis yields information about relatively few CpG sites. Of the 115 CpG sites found in the 8.7-kb *IL-4* gene, only 14 fall within a *Hpa*II restriction site. Hence, we investigated CpG methylation status in more detail using bisulfite modification and sequencing. This procedure involves using sodium bisulfite to convert unmethylated, but not methylated, cytosine residues to uracil (31). Subsequent amplification and sequencing of the modified DNA enables one to distinguish the originally methylated cytosines from the unmethylated cytosines, which are amplified as thymines. The regions where *Hpa*II digestion patterns differed between the cell types (Fig. 2*D*) were amplified from BSM DNA from naive, Th1, and Th2 cells and fibroblasts, and the PCR products were sequenced both directly and after cloning, to obtain different but complementary sets of information. Direct sequencing of BSM-PCR products reveals the overall methylation status of the total population of input fragments, and whether or not the modification reaction (i.e., conversion of unmethylated cytosine to thymine) has proceeded to completion. Cloning the BSM-PCR amplimers and sequencing the plasmid insert reveals the methylation status of the CpG sites within a single DNA fragment. Sequencing several such clones reveals any variability in CpG methylation patterns within the population as well as any correlations between the methylation status of particular CpG sites.

Seven CpG sites (Fig. 3*A*, numbered 1–7) are located in the 318-bp region that encompasses the *IL-4* proximal promoter, the transcriptional start site, and the first exon. Direct sequencing of the BSM-PCR amplimers (Fig. 3*C*) shows that the CpG sites in the first *IL-4* exon of T cells are predominantly methylated (i.e., remain unconverted; Fig. 3*C*, *lanes C*). By contrast, in the Th2 DNA sequence of the *IL-13* promoter (see Fig. 7*C*) the T and C bands of CpG sites 4 and 5 are of similar intensity, indicating that these cytosines are methylated in only approximately half the DNA fragments. These findings are in good agreement with the sequences of the individual cloned fragments of amplified DNA (Fig. 3*B*), which confirms the validity of both methods. Furthermore, the variety of CpG methylation patterns observed in the cloned fragments suggests that a representative population of the modified DNA molecules is amplified.

The seven CpG sites in the *IL-4* promoter and first exon are predominantly methylated in all three T cell populations, which suggests that demethylation of CpG sites around the *IL-4* promoter is not required for IL-4 expression in T cells. This region was also largely methylated in fibroblasts. We also used BSM PCR and sequencing to analyze the region in intron 2 that coincided with Th2-specific DHS I and II. Nine CpG sites are found in this region (Fig. 4*A*), two of which correspond to the *Hpa*II sites highlighted by an asterisk in Fig. 2*D*. In contrast to the region around the *IL-4* promoter, partial demethylation of CpG sites was seen after Th2, but not Th1, differentiation. Eighty percent of the Th2 DNA fragments had at least one unmethylated CpG site, compared with only 30–40% of the $CD45RA^+$ and Th1 DNA fragments. Furthermore, CpG sites 1 and 9, which are close to the Th2-specific DHS I and II, were both unmethylated in over half the Th2-derived fragments (Fig. 4*C*). Most of the fragments that were unmethylated at CpG site 1 were also unmethylated at CpG site 9. The unmethylated CpG sites in the Th1-derived fragments may result from a small minority of cells that might be capable of expressing IL-4, although our findings that CpG methylation patterns can differ between cells in a population are consistent with those of Fitzpatrick et al. (21), which showed that clonal heterogeneity is a prominent feature of cytokine expression in primary T cells.

This entire region was largely unmethylated in fibroblasts. Because the *IL-4* CpG methylation findings in fibroblasts were unexpected, we confirmed them by both *Msp*I/*Hpa*II digestion and

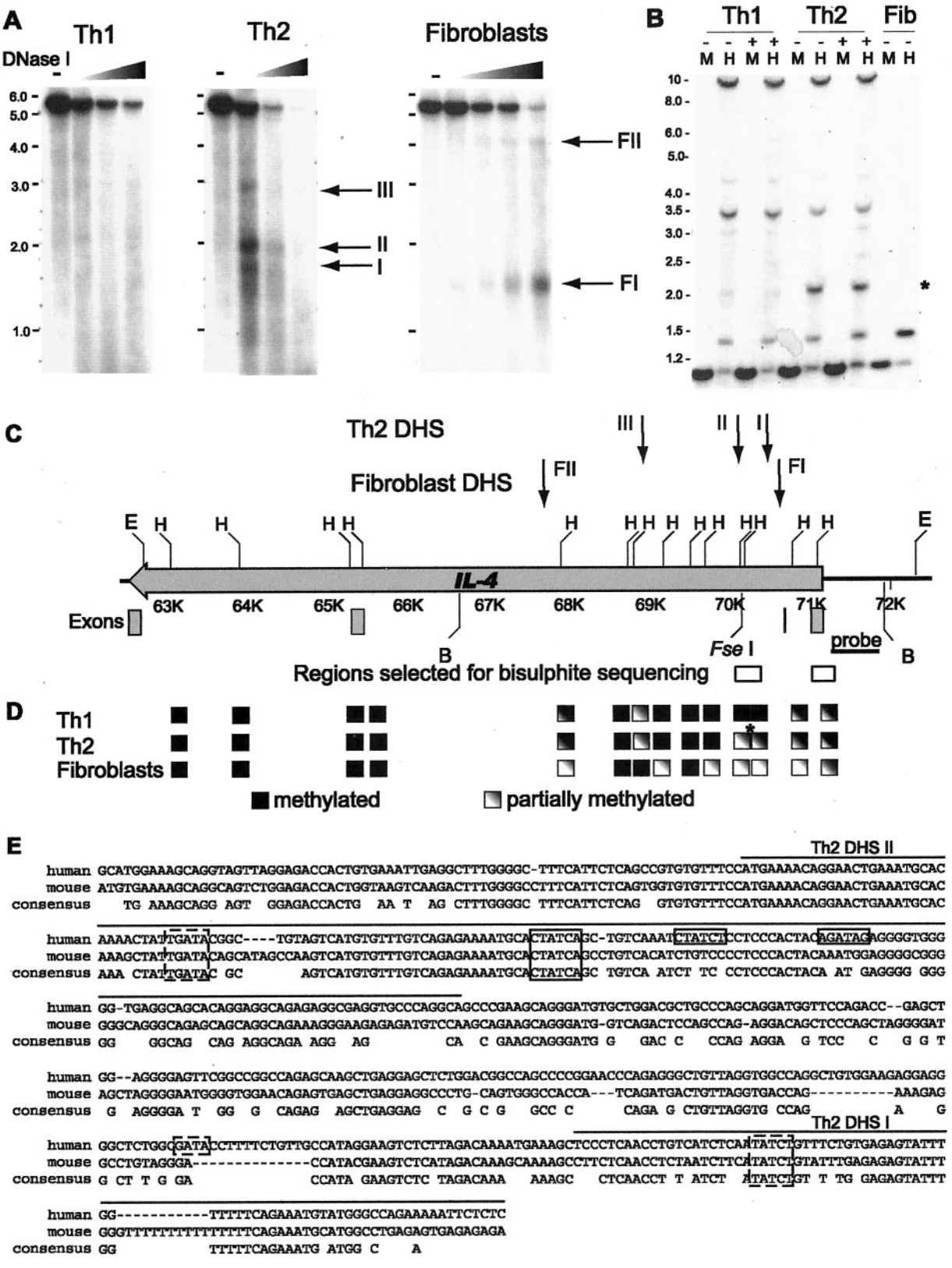

FIGURE 2. DHS and *Hpa*II digestion analysis in *IL-4*. *A*, Southern blots showing DHS analysis in *Bcl*I-digested genomic DNA from Th1 and Th2 cells and fibroblasts. Fragment size is indicated in kilobases to the *left* of the panels, horizontal arrows on the *right* denote DHS. Shaded triangles *above* the blots denote the use of increasing amounts of DNase I, and "−" denotes its absence. *B*, Southern blot of *Eco*RI-, *Msp*I (M)-, and *Hpa*II (H)-digested genomic DNA from unactivated (−) and activated (+) Th1 and Th2 cells and from unactivated (−) fibroblasts. Fragment size is indicated in kilobases to the *left* of the autoradiograph. *C*, Schematic diagram of *IL-4*, showing the positions of *Eco*RI (E), *Hpa*II (H), and *Bcl*I (B) digestion sites and the hybridization probe used in the Southern blots shown in *A* and *B*. Vertical arrows *above* the map show the location of DHS observed in Th2 cells and fibroblasts. *D*, Boxes show methylation status of CpG sites that fall within the *Hpa*II restriction sites located directly *above* them in *C*. *E*, DNA sequence around human Th2 DHS I and II (denoted by solid lines *above* the sequence), aligned with the syntenic murine sequence. Sequence identity (consensus) is shown *below*. Solid boxes indicate consensus GATA binding sites (WGATAR, where W is A or T and R is A or G) and dashed boxes indicate nonconsensus potential GATA sites.

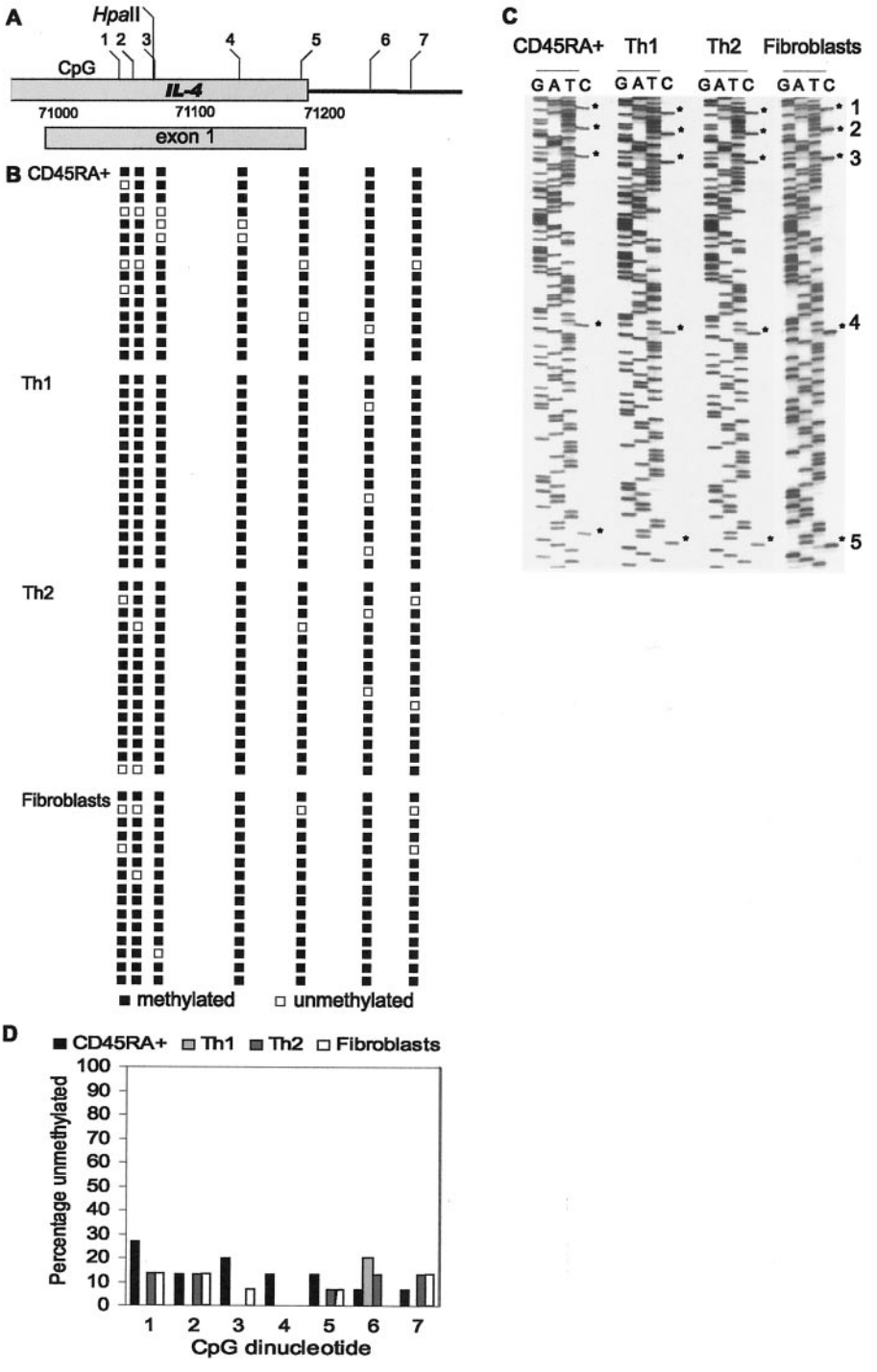

FIGURE 3. CpG methylation status in the *IL-4* promoter and first exon. *A*, Schematic diagram of the proximal promoter and first exon of *IL-4*, indicating relative positions of CpG and *Hpa*II sites. *B*, Methylation status of the CpG sites from individual BSM DNA fragments cloned from CD45RA$^+$, Th1 and Th2 cells, and fibroblasts. *C*, Autoradiograph of directly sequenced PCR products amplified from CD45RA$^+$, Th1, Th2, and fibroblast BSM DNA. *D*, Graph summarizing the percentage of unmethylated CpG sites observed at each position in the 15 DNA fragments analyzed in *B*.

BSM sequencing in DNA from three individuals, at passage numbers ranging from 7 to 22 (data not shown). We found very few differences in methylation patterns, either among the three individuals or between passage numbers. Rare differences in the degree of methylation occurred at a single CpG site, rather than across an entire region, and were of the order of a 10–50% increase or decrease in methylation status (data not shown). A trend of consistently increased or decreased methylation changes with increasing passage was not observed.

In summary, the *IL-4* DNA methylation patterns in all four cell types (Figs. 2*D*, 3*B*, and 4*B*) show clearly that naive cell and Th1 cell DNA is predominantly methylated in *IL-4* and that, after Th2 differentiation, the DNA becomes demethylated only in the second intron at a region coinciding with DHS formation, which suggests that these two events are linked. Meanwhile, despite the unmethylated status of the fibroblast DNA across the 5′ half of *IL-4*, any correlation between DHS and CpG demethylation is absent, in contrast to the Th2 cells.

DHS and CpG methylation around CNS-1

Because recent reports suggested that CNS-1 might be a coordinate regulator of Th2 cytokine expression (14, 15), we examined this region for chromatin and CpG methylation changes. In differentiated Th2 cells, two DHS were observed between CNS-1 and *IL-13* (Fig. 5*A*, *middle panel*, and *C*, designated I and II); in Th1

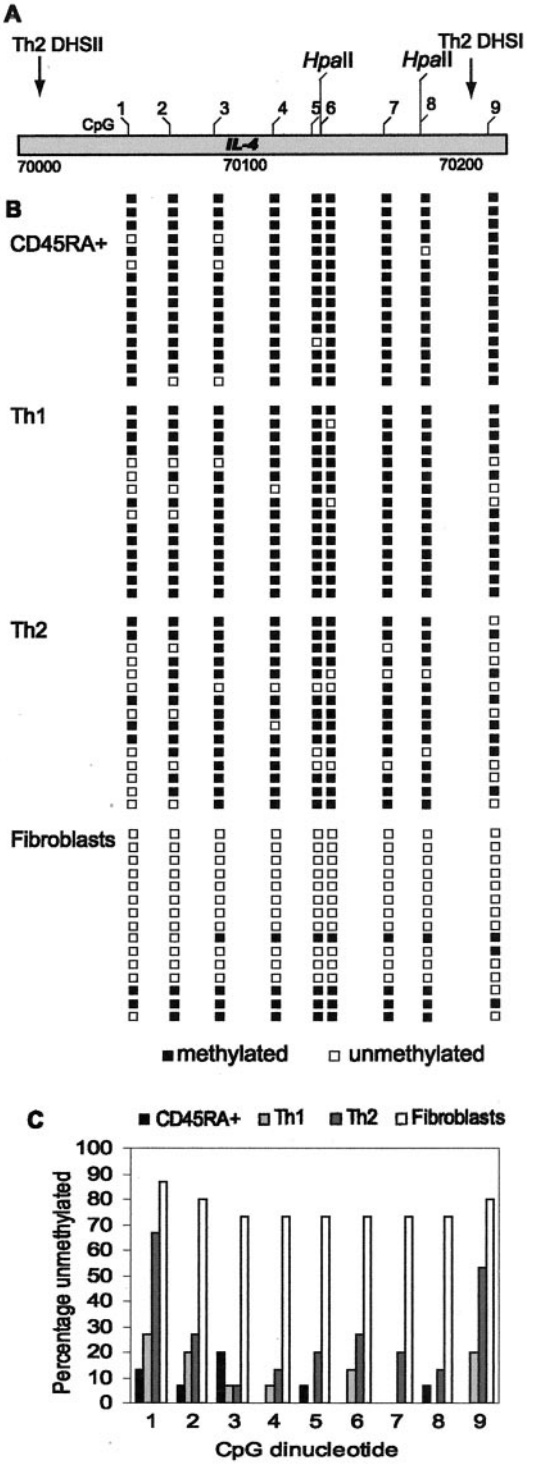

FIGURE 4. CpG methylation in the Th2-specific DHS region of the *IL-4* second intron. *A*, Schematic diagram of the region encompassing Th2-specific DHS (vertical arrows) in intron 2 of *IL-4*, indicating relative positions of CpG and *Hpa*II sites. *B*, Methylation status of the CpG sites from individual BSM DNA fragments cloned from CD45RA$^+$, Th1 and Th2 cells, and fibroblasts. *C*, Graph summarizing the percentage of unmethylated CpG sites observed at each position in the 15 DNA fragments analyzed in *B*.

cells the corresponding band is again considerably weaker. In fibroblasts, DHS designated FI and FII were also seen (Fig. 5*A*, *right panel*), one of which was located similarly to DHS I in Th2 cells. Unlike in the murine locus (17), DHS did not appear in CNS-1

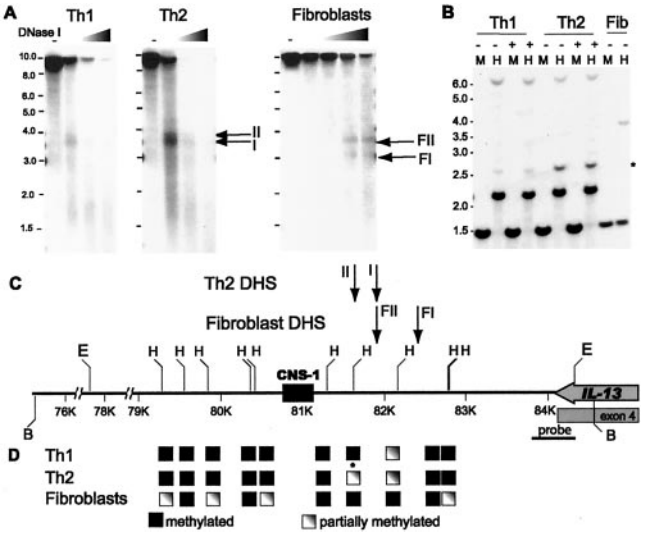

FIGURE 5. DHS and *Hpa*II digestion around CNS-1. *A*, Southern blots showing DHS analysis in *Bcl*I-digested genomic DNA from Th1 and Th2 cells and fibroblasts. Fragment size is indicated in kilobases to the *left* of the panels; horizontal arrows on the *right* denote DHS. Shaded triangles *above* the blots denote the use of increasing amounts of DNase I; "−" denotes its absence. *B*, Southern blot of *Eco*RI-, *Msp*I (M)-, and *Hpa*II (H)-digested genomic DNA from unactivated (−) and activated (+) Th1 and Th2 cells and from unactivated (−) fibroblasts. Fragment size is indicated in kilobases on the *left*. *C*, Schematic diagram of the CNS-1 region, showing the positions of *Eco*RI (E), *Hpa*II (H), and *Bcl*I (B) digestion sites, and the hybridization probe used in the Southern blots shown in *A* and *B*. Vertical arrows *above* the map show the location of DHS observed in Th2 cells and fibroblasts. *D*, Boxes show the methylation status of the CpG sites that fall within the *Hpa*II restriction sites located directly *above* them in *C*.

itself: the Th2 DHS are ~500 bp away from this conserved region in the direction of *IL-13*. No DHS were found between *IL-4* and this region in differentiated Th1 or Th2 cells or fibroblasts (data not shown).

To investigate CpG methylation status in this region, *Hpa*II digestion was performed (Fig. 5, *B* and *D*). Of the 10 *Hpa*II sites within the 6.5-kb *Eco*RI fragment that includes CNS-1, eight were totally methylated in Th1 and Th2 cells (Fig. 5*D*). One *Hpa*II site, which coincided with DHSII, was less methylated in Th2 cells than Th1 cells (Fig. 5, *B* and *D*, ∗). Once again, the unmethylated CpG site coincided with DHS formation. As in the *IL-4* gene, the fibroblasts were unmethylated at more CpG sites than were the T cells, and unmethylated sites did not correspond with DHS. Bisulfite sequencing analysis of DNA within CNS-1 showed that the CpG sites here were completely methylated in naive and Th1 cells and 90–95% methylated in Th2 cells (data not shown).

DHS and CpG methylation around IL-13

In resting Th2 cells, a DHS was observed at the transcription start site of *IL-13* (Fig. 6*A*, *middle panel*, and *B*, DHSIII). In Th1 cells, a very weak corresponding band was also observed. Again, GATA-3 binding sites are located within this DHS (Fig. 6*C*). Two other DHS (I and II) were seen in Th2 cells in the CpG-rich region that lies ~1 kb upstream of *IL-13*. DHS I is located within a CpG island and corresponds to a sequence that is conserved between the murine and human sequences (34). In fibroblasts, DHS FII coincided with Th2 DHS I in the CpG island, and another DHS, designated FI, was located 1 kb further upstream of *IL-13*, between the CpG island and an *Alu* repeat (Fig. 6*A*, *right panel*, and *B*).

The 2.5-kb CpG-rich region located ~1 kb upstream of *IL-13* contains both a CpG island (as defined by Gardiner-Garden and

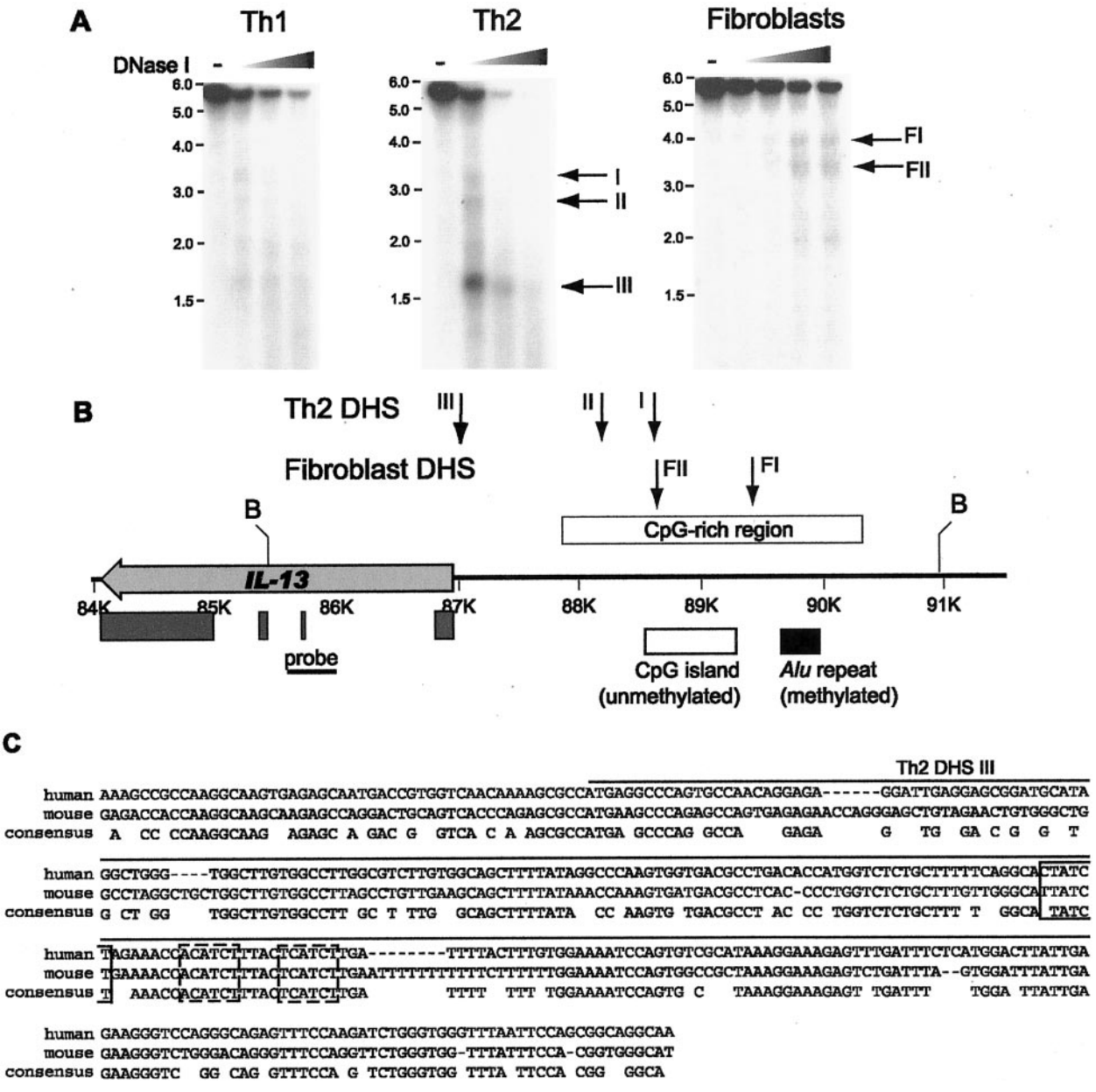

FIGURE 6. DHS around *IL-13*. *A*, Southern blots showing DHS analysis in *Bcl*I-digested genomic DNA from Th1 and Th2 cells and fibroblasts. Fragment size is indicated in kilobases to the *left* of the panels; horizontal arrows on the *right* denote DHS. Shaded triangles *above* the blots denote the use of increasing amounts of DNase I; "−" denotes its absence. *B*, Schematic diagram of *IL-13*, showing the positions of *Bcl*I (B) digestion sites, the exons as gray rectangles *below* the gene, and the position of the hybridization probe used in the Southern blots in *A*. The CpG-rich region is shown as a pale gray rectangle *above* the line, and the CpG island and *Alu* repeat found within this region are shown *below* the line. Vertical arrows *above* the map show the location of DHS observed in Th2 cells and fibroblasts. *C*, DNA sequence around human Th2 DHS I and II (denoted by solid lines *above* the sequence), aligned with the syntenic murine sequence. Sequence identity (consensus) is shown *below*. Solid boxes indicate consensus GATA binding sites (WGATAR, where W is A or T and R is A or G) and dashed boxes are nonconsensus potential GATA sites, as described by Kishikawa et al. (34).

Frommer in Ref. 35) and an *Alu* repeat (Fig. 6*B*). Initially, *Hpa*II digestion analysis of the CpG methylation status around *IL-13* was attempted, but the many fragments generated by the abundant *Hpa*II sites in the CpG-rich region complicated analysis of the data. Consequently, bisulfite modification and sequencing of the CpG-rich region was performed, which confirmed that, in all four cell types used in this study, all the CpG sites were unmethylated in the CpG island but methylated in the *Alu* repeat (data not shown). The methylation status of the CpG sites between the CpG island and the *Alu* repeat was variable.

The discovery of the Th2-specific DHS III prompted us to investigate the methylation status of the CpG sites around the transcriptional start site of *IL-13* in T cells and in fibroblasts. The region that was amplified contains seven CpG sites (Fig. 7*A*).

DNA from Th2 cells was largely unmethylated, unlike the *IL-4* promoter: 87% of Th2-derived fragments were unmethylated in at least one CpG site, compared with 53% of Th1-derived DNA fragments and only 27% of naive cell-derived fragments. Demethylation in the Th2 cells occurred mainly at CpG sites 4–7 (Fig. 7, *B* and *D*), which are found in the IL-13 proximal promoter. Moreover, all four sites were demethylated in half the cloned DNA fragments. This finding is analogous to that of Fitzpatrick and colleagues (21, 22), where bisulfite sequencing of the *IFN-γ* promoter in $CD8^+$ cells showed that demethylation at CpG sites was more

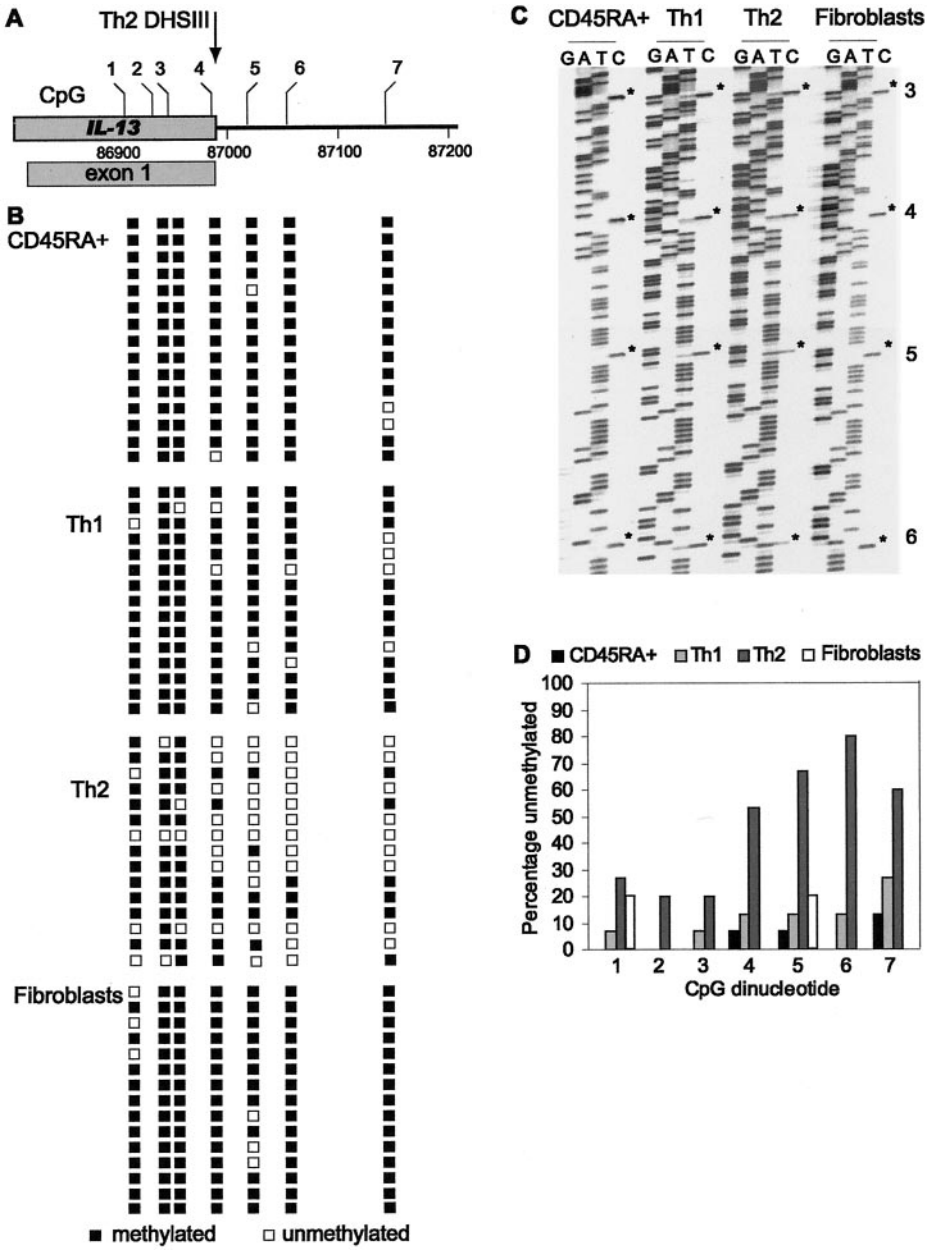

FIGURE 7. CpG methylation in the *IL-13* promoter and first exon. *A*, Schematic diagram of the proximal promoter and first exon of *IL-13*, indicating relative positions of CpG sites. *B*, Methylation status of the CpG sites from individual BSM DNA fragments cloned from $CD45RA^+$, Th1 and Th2 cells, and fibroblasts. *C*, Autoradiograph of directly sequenced PCR products amplified from $CD45RA^+$, Th1, Th2, and fibroblast BSM DNA. *D*, Graph summarizing the percentage of unmethylated CpG sites observed at each position in the 15 DNA fragments analyzed in *B*.

likely to occur upstream of the transcriptional start site. CpG demethylation and DHS formation at the transcriptional start site of *IL-13* thus coincide with the ability to express this gene in T cells. Direct sequencing of the fibroblast BSM-PCR products revealed that these CpG sites are predominantly methylated in fibroblasts (Fig. 7*C*); this was confirmed by sequencing cloned individual DNA fragments (Fig. 7*B*).

Discussion

We used an in vitro differentiation system to investigate the epigenetic and chromatin structure changes around human *IL-4* and *IL-13* that accompany Th1 and Th2 differentiation from naive precursors. After Th2 differentiation, CpG demethylation coincides with DHS formation at consensus GATA binding sites and is not the locus-wide event reported in the murine locus (25). The presence of DHS and high levels of CpG demethylation in *IL-4* and around CNS-1 in nonexpressing fibroblasts is also of interest.

We discovered several Th2-specific DHS around *IL-4* and *IL-13* in resting human Th2 cells after 14 days of differentiation (Fig. 8*A*). In *IL-4*, Th2-specific DHS appeared in the second intron and were absent in the promoter. Several GATA-3 consensus binding sites are present at DHS I and II, and Th2-specific CpG demethylation in the *IL-4* gene was observed only in this region (Fig. 2). Although there is a high level of conservation between the human and murine DNA sequences in this region, it is interesting that not all the GATA-3 sites are conserved between the species: two of the consensus binding sites are present only in the human sequence (Fig. 2*E*). It is likely that *IL-4* DHS I and II define an enhancer in human Th2 cells. Similar Th2-specific DHS have been observed in the second intron of the murine *IL-4* gene (Fig. 8*B*, HSII) (16) in a region found to be a weak *IL-4* enhancer in transgenic mice (36). These DHS and others around *IL-13* could be induced by ectopic GATA-3 expression in murine Th1 cells (12, 37). Studies in murine mast cells also identified a mast cell-specific *IL-4* DHS with enhancer function (38). This enhancer is activated by the mast cell-specific transcription factors GATA-1, GATA-2, and PU.1 (39) and it plays a role in establishing and maintaining *IL-4* CpG demethylation in IL-4-expressing mast cells, but only in the presence of intact GATA binding sites (40). The connection between

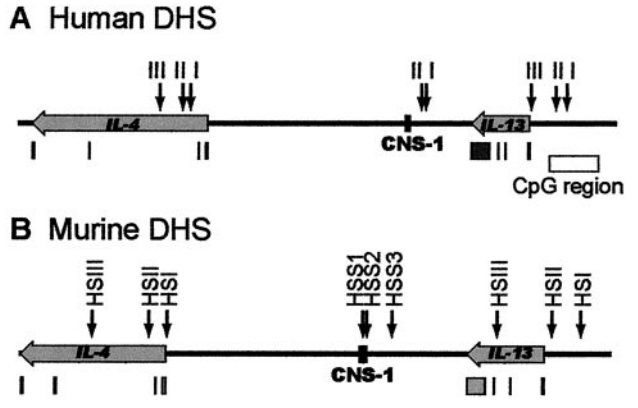

FIGURE 8. Relative positions of human and murine Th2-specific DHS. *A*, Schematic diagram of human *IL-4/IL-13* region; Th2-specific DHS observed in this study are denoted by vertical arrows. *B*, Schematic diagram of murine *IL-4/IL-13* region; the murine Th2-specific DHS observed by Takemoto et al. (17) and Agarwal and Rao (16) are denoted by vertical arrows.

DHS formation and regulatory elements containing GATA sites was suggested after GATA-1 was shown to break DNA/histone contacts when bound to nucleosomal DNA (41). GATA family members associate with CREB-binding protein, and CREB-binding protein is an acetyltransferase that acetylates not only histones (acetylated histones are a characteristic feature of transcriptionally active chromatin) but also GATA proteins (42–45). The fact that GATA sites were required to establish and maintain CpG demethylation in murine mast cells (40) may provide a link between the consensus GATA binding sites, DHS formation, and CpG demethylation that we observed in human Th2 cells.

In the human *IL-13* gene, the Th2-specific DHS I and III coincided with regions of sequence that are conserved between mice and humans (Fig. 6*C* and Ref. 34). DHSIII is located at the *IL-13* promoter, where three potential GATA-3 binding sites are located (Fig. 6). In murine Th2 cells, these sequences, which are conserved in humans, were required for cell-specific, GATA-3-driven expression of IL-13 in overexpression studies (34). We also observed that the three CpG sites (Fig. 7, labeled 5, 6 and 7) located near the GATA-3 binding sites were generally unmethylated in the human Th2 cells, but that DHS or CpG demethylation of the *IL-13* promoter were not seen in fibroblasts. This suggests that CpG demethylation and DHS formation around the GATA-3 sites at the *IL-13* promoter are required for IL-13 expression. Whether CpG demethylation plays a direct role in *IL-4/IL-13* transcriptional regulation or is merely a consequence of GATA-3-driven DHS formation requires further functional studies.

We also observed fibroblast-specific DHS that were distinct from Th2-specific DHS. From this we infer that genes that are not expressed in a particular tissue are not necessarily always free of DHS. Indeed, the presence of DHS in chromatin that is otherwise DNase I insensitive has been reported previously (46). We have not yet performed functional studies on any of the DNase I-hypersensitive elements that were identified in either Th2 cells or fibroblasts, but it is possible, given the transcriptional silence of the *IL-4* in fibroblasts, that the fibroblast-specific DHS in the second intron of *IL-4* may indicate a silencer or an insulator. Many intron-located silencers have been identified (47), including one in the first intron of the *CD4* gene, which represses promoter activity in $CD4^+$ T cells but not in $CD8^+$ T cells (48, 49). Alternately, the presence of DHS in fibroblasts may suggest a functionally defined chromatin structure that may be relevant to the maintenance of the expression of the other genes (e.g., *RAD50* or *KIF3A*) in the cluster. The absence of the Th2-specific transcription factor GATA-3 suggests a different mechanism of DHS formation in this nonhemopoietic lineage.

The CpG sites in the 5′ half of the fibroblast *IL-4* gene were also largely demethylated (Fig. 3*A*). The contrast between these findings and those in murine fibroblast cell lines (16), which showed that the DNA across the *IL-4*, *IL-5*, and *IL-13* genes was methylated in this cell type, may be because we used nontransformed, nonimmortalized fibroblasts from normal human skin: immortalized cell lines have been shown to be hypermethylated at nonessential genes (50). The presence of unmethylated CpG sites in *IL-4* in a differentiated cell type that does not express the gene (i.e., fibroblasts) suggests that another, tissue-specific process maintains its suppression. Alternatively, perhaps CpG methylation in a tissue that lacks Th2-specific factors may not be relevant to the regulation of this gene. It might thus be possible that CpG methylation in *IL-4* and *IL-13* could be a mechanism of suppression in potentially permissive lineages like naive and Th1 cells.

In conclusion, these data confirm that chromatin structure in this locus differs between human naive and Th1 cells, and Th2 cells. The appearance of Th2-specific DHS coincides with Th2-specific CpG demethylation (Figs. 2, *B* and *D*, 5, *B* and *D*, and 7, ∗), and both DHS formation and CpG demethylation occur near consensus GATA binding sites in *IL-4* and *IL-13*. CpG sites that are not in the vicinity of DHS remain methylated after differentiation to the Th2 phenotype. It will be interesting to see whether the recruitment of chromatin-modifying activities by GATA-3 is responsible for the DHS formation and CpG demethylation that we observed. Meanwhile, different patterns of DHS and unmethylated CpG sites are seen in the fibroblast *IL-4/IL-13* cluster and the link between DHS formation and CpG demethylation is absent, which suggests that chromatin structure and DNA methylation play different roles in *IL-4/IL-13* regulation in nonhemopoietic cells from those in lymphocytes.

Acknowledgments

We are grateful to Ian Kirby and John Newell-Price for technical assistance, to Tak Lee for support and encouragement, to Paul Lavender, Joan Boyes, and Patrick Varga-Weisz for critical review of the manuscript, and to Richard Meehan and Kasia Hawrylowicz for helpful discussions.

References

1. Abbas, A. K., K. M. Murphy, and A. Sher. 1996. Functional diversity of helper T lymphocytes. *Nature 383:787.*
2. Mosmann, T. R., and R. L. Coffman. 1989. TH1 and TH2 cells: different patterns of lymphokine secretion lead to different functional properties. *Annu. Rev. Immunol. 7:145.*
3. Robinson, D. S. 2000. Th-2 cytokines in allergic disease. *Br. Med. Bull. 56:956.*
4. Glimcher, L. H., and K. M. Murphy. 2000. Lineage commitment in the immune system: the T helper lymphocyte grows up. *Genes Dev. 14:1693.*
5. Szabo, S. J., S. T. Kim, G. L. Costa, X. Zhang, C. G. Fathman, and L. H. Glimcher. 2000. A novel transcription factor, T-bet, directs Th1 lineage commitment. *Cell 100:655.*
6. Mullen, A. C., F. A. High, A. S. Hutchins, H. W. Lee, A. V. Villarino, D. M. Livingston, A. L. Kung, N. Cereb, T. P. Yao, S. Y. Yang, and S. L. Reiner. 2001. Role of T-bet in commitment of TH1 cells before IL-12-dependent selection. *Science 292:1907.*
7. Murphy, K. M., W. Ouyang, J. D. Farrar, J. Yang, S. Ranganath, H. Asnagli, M. Afkarian, and T. L. Murphy. 2000. Signaling and transcription in T helper development. *Annu. Rev. Immunol. 18:451.*
8. Ho, I. C., M. R. Hodge, J. W. Rooney, and L. H. Glimcher. 1996. The proto-oncogene c-maf is responsible for tissue-specific expression of interleukin-4. *Cell 85:973.*
9. Zheng, W., and R. A. Flavell. 1997. The transcription factor GATA-3 is necessary and sufficient for Th2 cytokine gene expression in CD4 T cells. *Cell 89:587.*
10. Kim, J. I., I. C. Ho, M. J. Grusby, and L. H. Glimcher. 1999. The transcription factor c-Maf controls the production of interleukin-4 but not other Th2 cytokines. *Immunity 10:745.*
11. Zhang, D. H., L. Cohn, P. Ray, K. Bottomly, and A. Ray. 1997. Transcription factor GATA-3 is differentially expressed in murine Th1 and Th2 cells and controls Th2-specific expression of the interleukin-5 gene. *J. Biol. Chem. 272:21597.*

12. Lee, H. J., N. Takemoto, H. Kurata, Y. Kamogawa, S. Miyatake, A. O'Garra, and N. Arai. 2000. GATA-3 induces T helper cell type 2 (Th2) cytokine expression and chromatin remodeling in committed Th1 cells. *J. Exp. Med. 192:105*.
13. Frazer, K. A., Y. Ueda, Y. Zhu, V. R. Gifford, M. R. Garofalo, N. Mohandas, C. H. Martin, M. J. Palazzolo, J. F. Cheng, and E. M. Rubin. 1997. Computational and biological analysis of 680 kb of DNA sequence from the human 5q31 cytokine gene cluster region. *Genome Res. 7:495*.
14. Loots, G. G., R. M. Locksley, C. M. Blankespoor, Z. E. Wang, W. Miller, E. M. Rubin, and K. A. Frazer. 2000. Identification of a coordinate regulator of interleukins 4, 13, and 5 by cross-species sequence comparisons. *Science 288: 136*.
15. Mohrs, M., C. M. Blankespoor, Z. E. Wang, G. G. Loots, V. Afzal, H. Hadeiba, K. Shinkai, E. M. Rubin, and R. M. Locksley. 2001. Deletion of a coordinate regulator of type 2 cytokine expression in mice. *Nat. Immunol. 2:842*.
16. Agarwal, S., and A. Rao. 1998. Modulation of chromatin structure regulates cytokine gene expression during T cell differentiation. *Immunity 9:765*.
17. Takemoto, N., N. Koyano-Nakagawa, T. Yokota, N. Arai, S. Miyatake, and K. Arai. 1998. Th2-specific DNase I-hypersensitive sites in the murine IL-13 and IL-4 intergenic region. *Int. Immunol. 10:1981*.
18. Keshet, I., J. Lieman-Hurwitz, and H. Cedar. 1986. DNA methylation affects the formation of active chromatin. *Cell 44:535*.
19. Mostoslavsky, R., N. Singh, A. Kirillov, R. Pelanda, H. Cedar, A. Chess, and Y. Bergman. 1998. κ chain monoallelic demethylation and the establishment of allelic exclusion. *Genes Dev. 12:1801*.
20. Whitehurst, C. E., M. S. Schlissel, and J. Chen. 2000. Deletion of germline promoter PDβ1 from the TCRβ locus causes hypermethylation that impairs Dβ1 recombination by multiple mechanisms. *Immunity 13:703*.
21. Fitzpatrick, D. R., K. M. Shirley, L. E. McDonald, H. Bielefeldt-Ohmann, G. F. Kay, and A. Kelso. 1998. Distinct methylation of the interferon γ (IFN-γ) and interleukin 3 (IL-3) genes in newly activated primary $CD8^+$ T lymphocytes: regional IFN-γ promoter demethylation and mRNA expression are heritable in $CD44^{high}CD8^+$ T cells. *J. Exp. Med. 188:103*.
22. Fitzpatrick, D. R., K. M. Shirley, and A. Kelso. 1999. Cutting edge: stable epigenetic inheritance of regional IFN-γ promoter demethylation in $CD44^{high}CD8^+$ T lymphocytes. *J. Immunol. 162:5053*.
23. Bird, J. J., D. R. Brown, A. C. Mullen, N. H. Moskowitz, M. A. Mahowald, J. R. Sider, T. F. Gajewski, C. R. Wang, and S. L. Reiner. 1998. Helper T cell differentiation is controlled by the cell cycle. *Immunity 9:229*.
24. Lee, P. P., D. R. Fitzpatrick, C. Beard, H. K. Jessup, S. Lehar, K. W. Makar, M. Perez-Melgosa, M. T. Sweetser, M. S. Schlissel, S. Nguyen, et al. 2001. A critical role for dnmt1 and DNA methylation in T cell development, function, and survival. *Immunity 15:763*.
25. Agarwal, S., J. P. Viola, and A. Rao. 1999. Chromatin-based regulatory mechanisms governing cytokine gene transcription. *J. Allergy Clin. Immunol. 103:990*.
26. Green, M. H., C. F. Arlett, J. Cole, S. A. Harcourt, A. Priestley, A. P. Waugh, G. Stephens, D. M. Beare, N. A. Brown, and G. A. Shun-Shin. 1991. Comparative human cellular radiosensitivity. III. Gamma-radiation survival of cultured skin fibroblasts and resting T-lymphocytes from the peripheral blood of the same individual. *Int. J. Radiat. Biol. 59:749*.
27. Rogan, D. F., D. J. Cousins, and D. Z. Staynov. 1999. Intergenic transcription occurs throughout the human IL-4/IL-13 gene cluster. *Biochim. Biophys. Acta 255:556*.
28. Cockerill, P. N. 2000. Identification of DNaseI hypersensitive sites within nuclei. *Methods Mol. Biol. 130:29*.
29. Stewart, A. F., A. Reik, and G. Schutz. 1991. A simpler and better method to cleave chromatin with DNase 1 for hypersensitive site analyses. *Nucleic Acids Res. 19:3157*.
30. Chanda, V. B. 1998. Preparation and analysis of DNA. In *Current Protocols in Molecular Biology*. Ausubel, M., R. Brent, R. E. Kingston, D. D. Moore, J. G. Seidman, J. A. Smith, and K. Struhl, eds. Wiley, New York p. 2.9.7.
31. Frommer, M., L. E. McDonald, D. S. Millar, C. M. Collis, F. Watt, G. W. Grigg, P. L. Molloy, and C. L. Paul. 1992. A genomic sequencing protocol that yields a positive display of 5-methylcytosine residues in individual DNA strands. *Proc. Natl. Acad. Sci. USA 89:1827*.
32. Clement, L. T. 1992. Isoforms of the CD45 common leukocyte antigen family: markers for human T-cell differentiation. *J. Clin. Immunol. 12:1*.
33. Hannet, I., F. Erkeller-Yuksel, P. Lydyard, V. Deneys, and M. DeBruyere. 1992. Developmental and maturational changes in human blood lymphocyte subpopulations. *Immunol. Today 13:215*.
34. Kishikawa, H., J. Sun, A. Choi, S. C. Miaw, and I. C. Ho. 2001. The cell type-specific expression of the murine *IL-13* gene is regulated by GATA-3. *J. Immunol. 167:4414*.
35. Gardiner-Garden, M., and M. Frommer. 1987. CpG islands in vertebrate genomes. *J. Mol. Biol. 196:261*.
36. Lee, G. R., P. E. Fields, and R. A. Flavell. 2001. Regulation of IL-4 gene expression by distal regulatory elements and GATA-3 at the chromatin level. *Immunity 14:447*.
37. Takemoto, N., Y. Kamogawa, H. Jun Lee, H. Kurata, K. I. Arai, A. O'Garra, N. Arai, and S. Miyatake. 2000. Cutting edge: chromatin remodeling at the IL-4/IL-13 intergenic regulatory region for Th2-specific cytokine gene cluster. *J. Immunol. 165:6687*.
38. Henkel, G., D. L. Weiss, R. McCoy, T. Deloughery, D. Tara, and M. A. Brown. 1992. A DNase I-hypersensitive site in the second intron of the murine IL-4 gene defines a mast cell-specific enhancer. *J. Immunol. 149:3239*.
39. Henkel, G., and M. A. Brown. 1994. PU.1 and GATA: components of a mast cell-specific interleukin 4 intronic enhancer. *Proc. Natl. Acad. Sci. USA 91:7737*.
40. Hural, J. A., M. Kwan, G. Henkel, M. B. Hock, and M. A. Brown. 2000. An intron transcriptional enhancer element regulates IL-4 gene locus accessibility in mast cells. *J. Immunol. 165:3239*.
41. Boyes, J., J. Omichinski, D. Clark, M. Pikaart, and G. Felsenfeld. 1998. Perturbation of nucleosome structure by the erythroid transcription factor GATA-1. *J. Mol. Biol. 279:529*.
42. Boyes, J., P. Byfield, Y. Nakatani, and V. Ogryzko. 1998. Regulation of activity of the transcription factor GATA-1 by acetylation. *Nature 396:594*.
43. Hung, H. L., J. Lau, A. Y. Kim, M. J. Weiss, and G. A. Blobel. 1999. CREB-binding protein acetylates hematopoietic transcription factor GATA-1 at functionally important sites. *Mol. Cell. Biol. 19:3496*.
44. Blobel, G. A., T. Nakajima, R. Eckner, M. Montminy, and S. H. Orkin. 1998. CREB-binding protein cooperates with transcription factor GATA-1 and is required for erythroid differentiation. *Proc. Natl. Acad. Sci. USA 95:2061*.
45. Yamagata, T., K. Mitani, H. Oda, T. Suzuki, H. Honda, T. Asai, K. Maki, T. Nakamoto, and H. Hirai. 2000. Acetylation of GATA-3 affects T-cell survival and homing to secondary lymphoid organs. *EMBO J. 19:4676*.
46. Forrester, W. C., L. A. Fernandez, and R. Grosschedl. 1999. Nuclear matrix attachment regions antagonize methylation-dependent repression of long-range enhancer-promoter interactions. *Genes Dev. 13:3003*.
47. Ogbourne, S., and T. M. Antalis. 1998. Transcriptional control and the role of silencers in transcriptional regulation in eukaryotes. *Biochem. J. 331:1*.
48. Donda, A., M. Schulz, K. Burki, G. De Libero, and Y. Uematsu. 1996. Identification and characterization of a human CD4 silencer. *Eur. J. Immunol. 26:493*.
49. Zou, Y. R., M. J. Sunshine, I. Taniuchi, F. Hatam, N. Killeen, and D. R. Littman. 2001. Epigenetic silencing of CD4 in T cells committed to the cytotoxic lineage. *Nat. Genet. 29:332*.
50. Antequera, F., J. Boyes, and A. Bird. 1990. High levels of de novo methylation and altered chromatin structure at CpG islands in cell lines. *Cell 62:503*.